Nat. Hazards Earth Syst. Sci., 11, 613–625, 2011
www.nat-hazards-earth-syst-sci.net/11/613/2011/
doi:10.5194/nhess-11-613-2011

Natural Hazards and Earth System Sciences

Evolution of extreme Total Water Levels along the northern coast of the Iberian Peninsula

D. F. Rasilla Álvarez and J. C. García Codron

Gestión del Medio Natural, Departamento de Geografía, Urbanismo y Ordenación del Territorio, Universidad de Cantabria, Santander, Spain

Received: 20 June 2010 – Revised: 3 January 2011 – Accepted: 8 January 2011 – Published: 23 February 2011

Abstract. This paper assesses the evolution of storminess along the northern coast of the Iberian Peninsula through the calculation of extreme (1%) Total Water Levels (eTWL) on both observed (tide gauge and buoy data) and hindcasted (SIMAR-44) data. Those events were first identified and then characterized in terms of oceanographic parameters and atmospheric circulation features. Additionally, an analysis of the long-term trends in both types of data was performed. Most of the events correspond to a rough wave climate and moderate storm surges, linked to extratropical disturbances following a northern track. While local atmospheric conditions seem to be evolving towards lesser storminess, their impact has been balanced by the favorable exposure of the northern coast of the Iberian Peninsula to the increasing frequency and strength of distant disturbances crossing the North Atlantic. This evolution is also correctly reproduced by the simulated long-term evolution of the forcing component (meteorological sea level residuals and wave run up) of the Total Water Level values calculated from the SIMAR 44 database, since sea level residuals have been experiencing a reduction while waves are arriving with longer periods. Finally, the addition of the rate of relative sea level trend to the temporal evolution of the atmospheric forcing component of the Total Water Level values is enough to simulate more frequent and persistent eTWL.

1 Introduction

Coastal areas are among the most vulnerable areas of the Earth to global warming. Climate models predict a rise in the global mean sea level of between 0.18 m and 0.59 m from 1980–1999 to 2090–2099 (Meehl et al., 2007), and this sea-level rise could induce significant morphodynamic responses, such as shoreline migrations, beach erosion, flooding of existing low-lying coastal plains, increased salinity of aquifers, and changes in sediment and nutrient transport (Crooks, 2004; FitzGerald et al., 2008). Biodiversity will also be threatened by the loss of coastal forests (Williams et al., 1999, 2003; Desantis et al., 2007), saltmarshes (Denslow and Battaglia, 2002) and coral reef bleaching (Jokiel and Brown, 2004). From the human point of view, approximately 10% of the world population currently lives in low-elevation coastal zones, including at least two-thirds of the world's largest cities. If such changes occur, they will be accompanied by extensive damages to infrastructure, affectation of coastal uses and resources and loss of goods and services (Costanza et al., 1997; Schrötter et al., 2005; Michael, 2007). Since the largest impacts will probably occur in developing countries, where there is a lack of resources for mitigation, great political and economical stresses are also expected in poorer states (Turner et al., 1996).

Observed changes in the frequency, strength and trajectories of the storms (Kushnir et al, 1997; WASA Group, 1998; Wang and Swail, 2001; Méndez et al., 2006) usually control spatial and temporal variability in the frequency and intensity of wave energy and storm surges, which in turn are the processes responsible for the most active morphogenetic events. As they make the local sea level rise above ordinary levels, overtopping beaches, dune ridges or coastal defences, such processes can regionally intensify the impact of the global sea-level rise. An understanding of the relative importance of these climate-controlled processes and their inclusion in methodologies to assess the resulting risk of coastal hazards is critical to both guide future research programs and manage the coast soundly.

Correspondence to:
D. F. Rasilla Álvarez
(rasillad@unican.es)

Published by Copernicus Publications on behalf of the European Geosciences Union.

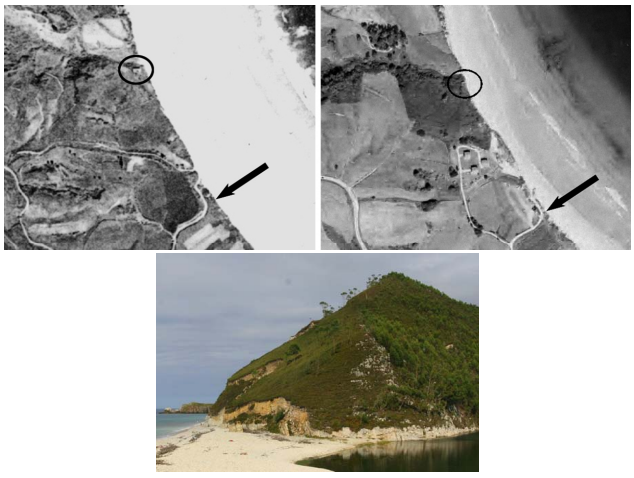

Fig. 1. Upper panel, coastline retreat at Oyambre beach (Cantabria). The physical reference points (building and road) indicate a retreat of several meters between 1956 and 1999 (Garrote and Garzón, 2004). Lower panel, collapses in quarcite cliffs, San Antolín de Bedón (Asturias).

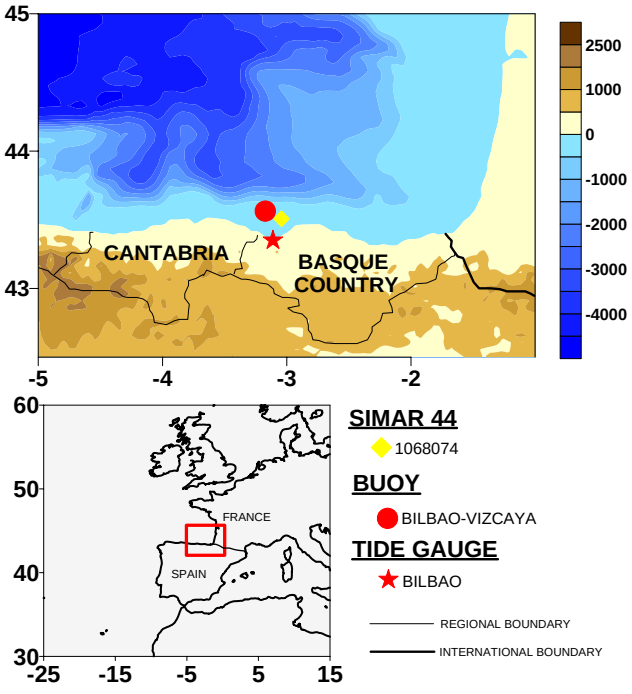

Fig. 2. Location of the study area and sources of information.

The northern coast of the Iberian Peninsula has suffered increasing human pressure over the last centuries, which sped up during the 20th century. The most transformed sector is the eastern area, the coast of Cantabria and the Basque country. Most of the towns are located in small bays, generally at the outlets of the rivers, but the remaining coast is escarped, dominated by resistant substrata which derived into vertical cliffs and abrasion platforms, intercalated by sandy beaches (Pascual et al., 2004; Borja and Collins, 2004). The continental shelf is extremely reduced with a mean width of 30 to 40 km. It is open to the westerly atmospheric circulation due to its orientation towards N and NW, and subjected to a semi-diurnal tide (González et al., 2004). The information available from tide gauge observations show that the average range is around 3 m, with maximums in excess of 4.90 m and minimums of 1.65 m (REDMAR, 2005). Analysis of tide gauge records from Santander recently confirmed by foraminifera transfer functions (Leorri and Cearreta, 2009), revealed that the relative mean sea-level rose at a rate of $2.08 \pm 0.33\,\mathrm{mm\,yr^{-1}}$ during the second half of the 20th century (Marcos et al., 2005), also undergoing an acceleration at the end of this period (Marcos et al., 2007). Wave energy levels display also remarkable seasonal variations, while wave direction remains rather constant throughout the year, with 75% coming from the fourth quadrant (W-NNW).

The main task of our research is to find out whether or not the evolution of the storminess along the coastline of Northern Iberian Peninsula during the 2nd half of the 20th century might be compatible with some evidence of current active erosion (Fig. 1). This task was accomplished first through the validation of some oceanographic parameters obtained from a simulated database compared with observed data. Later, most favourable oceanographic and atmospheric conditions for producing potentially extreme erosion events along the northern coast of the Iberian Peninsula are identified and characterized. Finally, the long term trends in both types of leading conditions are evaluated in order to explain the temporal evolution of the phenomena.

2 Data

Two different sources of information have been used in this contribution: instrumental data and numerical simulations of several atmospheric and oceanographic parameters. Within the instrumental data (Fig. 2), actual sea level heights, astronomical tides and atmospheric sea level residuals have been obtained from the tide gauge located inside the Bilbao harbour, belonging to the REDMAR network (Álvarez-Fanjul et al., 2001), while significant wave height and the wave peak period from the Bilbao buoy was also used (deep sea REDEXT network; depth 600 m). Both types of data have been provided by Puertos del Estado, which submitted those data to an initial quality control analysis to detect and eliminate anomalous data or low variability values. The instrument-based study focuses on fifteen years of simultaneous time series, from 1992 to 2008.

The analysis of long-term trends in parameters such as sea level heights or waves is difficult because of the lack of appropriate time series of instrumental observations. For example, buoy observations have only been available since 1990, when a national buoy network was installed, but the

instrumental data are usually incomplete due to periods of malfunctioning and other problems. Tide gauge data series are usually longer, but also suffer from a lack of homogeneity (changes of location, datum or devices). Hindcasted data offer longer, continuous and homogeneous records of the same magnitudes, thus our analysis of inter-annual variability back in time was based on a simulated database, the SIMAR 44, which is a subset of the long-term 44-year (1958–2001) HIPOCAS database (Guedes-Soares et al., 2002, Sotillo et al., 2005), also provided by Puertos del Estado. The HIPOCAS database has been used in several different research fields, such as wave energy assessment (Iglesias and Carballo, 2010), wind extremes (Sotillo et al., 2006), precipitation (Morata et al., 2008) and sea level regionalization (Sebastião et al., 2008). It is the result of an atmospheric hindcast performed by means of the regional atmospheric model REMO, covering the whole Mediterranean basin by a grid with a horizontal resolution of 0.5×0.5, with NCEP/NCAR global reanalysis used as initial and boundary conditions. Hourly pressure and wind fields calculated by REMO were used as input to the HAMSOM model (Álvarez et al., 1997), which provided sea level predictions, while wave parameters were obtained from a third generation wave model WAM (Hasselmann et al., 1988).

In the present paper, we use the SIMAR 44 closest node to the instrumental observations (node 1 068 074). Large-scale circulation data (sea level pressure and 10 m u and v wind fields) were obtained from the REANALYSIS/NCEP database (Kalnay et al., 1996). Several parameters related to cyclone life cycle (position, central pressure and local Laplacian at each cyclone centre) were retrieved from the Northern Hemisphere Cyclone Locations and Characteristics database (http://nsidc.org/data/docs/daac/nsidc0423_cyclone/). This data set comprises a 50-year record of daily extratropical cyclone statistics computed for the Northern Hemisphere. Cyclone locations and characteristics were obtained by applying the updated Serreze (1995) algorithm to daily Sea Level Pressure (SLP) data at six-hour intervals.

3 Methodology

The connection between potential coastal erosion and atmospheric and oceanographic variability has been established through calculation of the Total Water Level (henceforth TWL). This is a synthetic index which combines the sea level heights, run-up levels of the waves and beach morphology in the form of the foreshore beach slope (Ruggiero et al., 1996, 2001). It attempts to reproduce the frequency with which a particular backshore feature, such as the base or crest of a dune or toe of a sea cliff can be reached by the oceanic waters. Since the TWL is a function of several combined parameters, any trend or change in those magnitudes will directly influence the vulnerability of a particular coastal area to erosion. An estimation of the TWL can be achieved through the following equation

$$\mathrm{TWL} = Z_T + R_{2\%} \tag{1}$$

where Z_T is the measured sea level and $R_{2\%}$ is two percent exceedence value of wave run-up. The original approach was slightly modified by taking advantage of an updated empirical relation for extreme wave run-up derived from diverse field experiments (Stockdon et al., 2006). Estimates of the TWL using that formulation are applicable to natural beaches over a wide range of hydrodynamic and morphological conditions and can be written as

$$\mathrm{TWL} = Z_T + 1.1\left(0.35\tan\beta\,(H_0 L_0)^{1/2} + \frac{\left[H_0 L_0\left(0.563\tan\beta^2 + 0.004\right)\right]^{1/2}}{2}\right) \tag{2}$$

where $\tan\beta$ is the foreshore beach slope, H_0 is the offshore wave height, L_0 is the offshore wave length, given by linear theory as $(g/2\pi)T^2$ where g is the acceleration due to gravity and T is the peak wave period. Additionally, the measured sea level Z_t combines the astronomical tides and the atmospheric sea level residuals. Equation (2) can be applied anywhere with available measurements of waves, tides, and beach morphology (Ruggiero et al., 1997, 2004). Observed (1992–2008) and simulated (1958–2001) time series of TWL were constructed by computing 6-hourly $R_{2\%}$ values obtained from significant wave heights and peak periods, and adding 6-hourly sea water levels values, estimated from actual readings coming from buoy plus tide gauge data, and hindcasted data from SIMAR-44. Beach morphology along the northern coast of the Iberian Peninsula is diverse, due to local regimes of wave and tides. As we are not interested on TWL estimates for a specific beach but rather an overall estimation of potential erosion, a theoretical foreshore beach slope of 0.05 was used in this research. The 1% TWL values were identified as extreme TWL (eTWL) events, and the independence of each event was based on the "peak-over-threshold" technique (Goda, 1988). Instrumental (actual) observations will be used to identify the actual oceanographic and atmospheric environment linked to the eTWL; because the length of the instrumental record is quite short, long-term percentiles of Total Water Level were obtained from the application of Eq. (2) to the hindcasted time series of sea level residuals, significant wave height and peak period, in addition to the astronomical tide and the long term trend of sea level rising.

To characterize the atmospheric circulation conditions associated with extreme TWL events, composite fields of surface sea level pressure and 10 m u and v wind components as well as the distributions of regional atmospheric flow indices were derived. Compositing is a synoptic classification method involving the averaging of a set of maps that meet some specified criteria, useful as a "first attempt" at understanding a climatic dataset (Yarnal, 1993). The regional flow

indices were calculated following an objective scheme initially proposed by Jenkinson and Collison (1977) and based on the original manual Lamb weather types. In this classification scheme, whose only required input parameter is a gridded sea level pressure field, several magnitudes are obtained, namely average pressure, geostrophic wind speed and direction, and vorticity; besides, a dimensionless Gale index was defined (Eq. 3), considering the strength of directional flow (F) and vorticity (Z).

$$G = \left[F^2 + (0.5Z)^2\right]^{1/2} \quad (3)$$

Actual meteorological observations of wind and pressure were not considered, because of an analysis of the reliability of the data provided by several stations in the area that had detected different inhomogeneities, specially wind data, which might compromise the results of the analysis.

In addition to a simple linear regression, a trend analysis was also carried out on several oceanographic and meteorological parameters, applying the Mann-Kendall nonparametric statistical trend test in conjunction with Sen's slope estimator to obtain the magnitude of the trend. The MAKESENS macro used for this task (www.emep.int/assessment/MAKESENS_1_0.xls) provides the degree of significance of the Mann-Kendall test and two confidence intervals for the Sen's slope estimation, one with a significance of 99% (Qmin99 and Qmax99) and the other with a significance of 95% (Qmin95 and Qmax95).

4 Validation of SIMAR 44 database

An accurate assessment of the long-term variability of oceanographic quantities using simulated data requires a rigorous validation against observed data. Thus, in-situ tide gauge and buoy data were compared with the closest SIMAR 44 grid point to the reference data. For comparison purposes, observations (hourly frequency) and hindcasted (3-hourly sampling) data were re-sampled with the same temporal resolution as the NCEP reanalysis, i.e. 00:00, 06:00, 12:00 and 18:00 UTC. Regarding the sea level variability, only its meteorological component was considered, obtained after subtracting the astronomical tide from the observed sea level. This is called meteorological residual, due to the determinant role of the meteorological conditions in comparison to other non-periodic effects. Some statistics of agreement, i.e. the root mean square error (RMSE), the Bias and the correlation and regression coefficients, shown in Table 1, and the graphical comparison (Fig. 3) show a reasonable agreement between the values calculated by the model and the tide gauge measurements: typical values for RMSE are 6–7 cm and the correlation index was very high (>0.80). Most of the largest peaks were correctly reproduced, including relevant surge episodes, but some failures were detected. This shortcoming has been attributed to an underestimation of the wind fields when the wind blows offshore-wards through an abrupt orography change in the coastal region (Sotillo et al., 2005; Ratsimandresey et al., 2008).

Table 1. General statistics derived from the comparison between instrumental (tide gauge and buoy) and the SIMAR 44 database.

	r	RMSE	BIAS	Slope	Intercept	n
Sea level residual						
Bilbao	0.82	0.065	0.004	0.764	0.026	25 243
Wave parameters						
SWH	0.91	0.516	0.267	0.764	0.242	18 048
Tp	0.75	2.149	4.622	0.795	2.989	18 048

A comparison between the wave regime observed at the Bilbao buoy along with the corresponding waves simulated by SIMAR 44 at the closest grid point is presented in Fig. 4. The parameter that was most faithfully reproduced was the significant wave height, as the high correlation coefficient (0.92) evidences, the temporal variability being adequately simulated by the model, even during the roughest events. The results from the comparison regarding the wave period were less satisfactory, with a lower correlation value (0.75) and a larger dispersion.

5 Results

5.1 Characterization of extreme total water levels

The monthly frequency of eTWL events during the 1992–2008 instrumental period is shown in Fig. 5. Most of them occur between December and March (71% of all events), followed by an almost continuous decrease towards summer, when no event was reported. This concentration during the stormiest season of the year supports the assumption that atmospheric forcing processes, rather than sea level variations due to astronomical factors, play a fundamental role in the occurrence of these events.

Meteorological sea level residuals and wave conditions associated with eTWL events were also investigated in order to determine if they are different from the normal conditions and to get a better insight of the effects of the storms. The analysis of the magnitude of the residuals shows that most of the extreme TWL events are accompanied by a positive elevation of the sea level above the tide level (78%) but this elevation is relatively weak, since storm surges in excess of 20 cm represent only 20% of the total (Fig. 6).

The distribution of significant wave heights indicates rough conditions associated to eTWL, with an average height of 5 to 7 m in deep-water, instead of the normal 1–2 m given

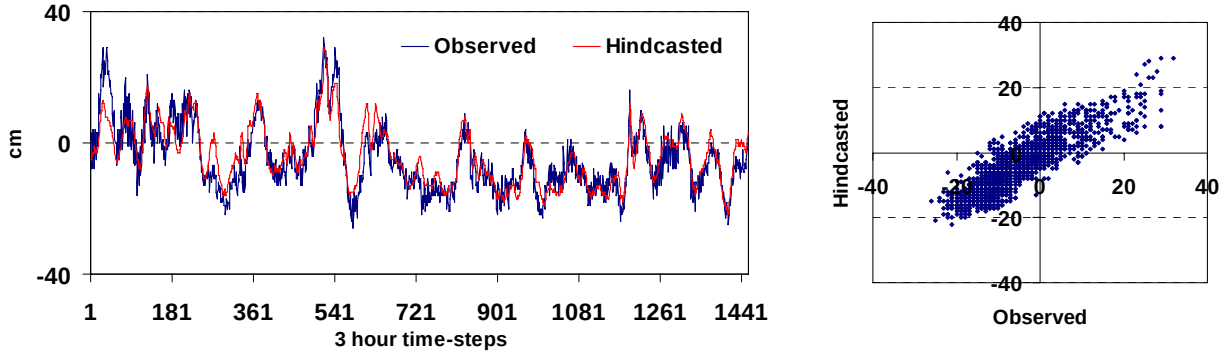

Fig. 3. Observed (Bilbao tide gauge) and hindcasted (SIMAR 44) time series (left) and scatterplot (right) of meteorological sea level residuals (measured sea level minus astronomical tide). Temporal resolution: 3 h (00:00, 03:00, 06:00, 09:00, 12:00, 15:00, 18:00 and 21:00 UTC) time steps from 1 October 1992 to 31 March 1993.

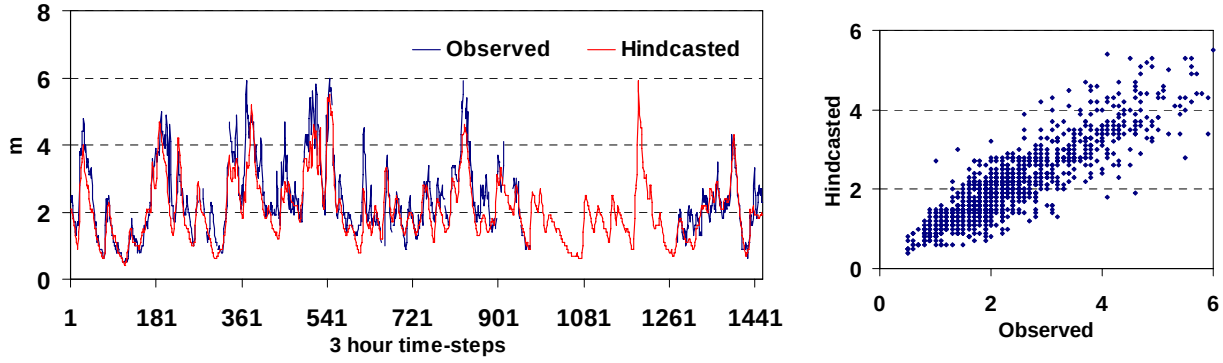

Fig. 4. Observed (Bilbao buoy) and hindcasted (SIMAR 44) time series (left) and scatterplot (right) of significant wave height. Temporal resolution: 3 h (00:00, 03:00, 06:00, 09:00, 12:00, 15:00, 18:00 and 21:00 UTC) time steps from 1 October 1992 to 31 March 1993.

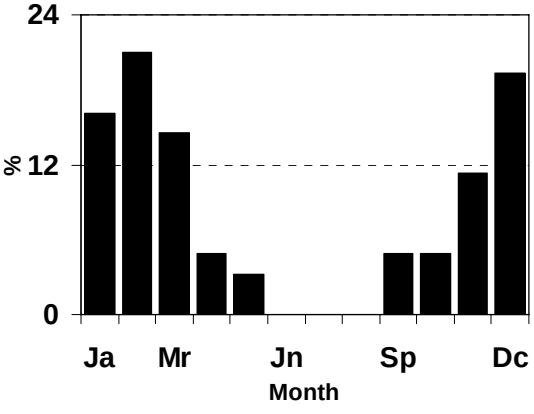

Fig. 5. Monthly frequency of occurrence of eTWL events derived from instrumental data (1992–2008).

by the climatology analysis. Similar distribution is observed in relation to peak periods in which the dominant class corresponds to 15 s, with a secondary maximum of 13 s, while the average wave period is approximately 10 s (Fig. 7).

5.2 Large-scale circulation conditions associated with extreme TWL events

Figures 6 and 7 highlight the fact that most eTWL events are strongly dependent on anomalous wave events, rather than extreme surge events. Both processes share the same atmospheric forcing, the combined action of atmospheric pressure and wind stress on the sea surface which are closely related to cyclones, but their relevance depends on the geographical characteristics of the coastal region. In the case of storm surges, the atmospheric pressure produces what is called the inverse barometric effect, according to which, in steady conditions the sea level increases when a low pressure area approaches. Additionally, wind stress pushes the water column horizontally and accumulates it at the closed end of a basin, the slope of the sea surface being proportional to wind stress and to the inverse of the water depth. Therefore, the inverse barometer should be more effective in open and deep waters, such as the coast of northern Spain, while the action of wind stress dominates in shallow waters. Bearing in mind the short continental shelf of the northern Iberian margin, the relatively weak values of the meteorological sea level

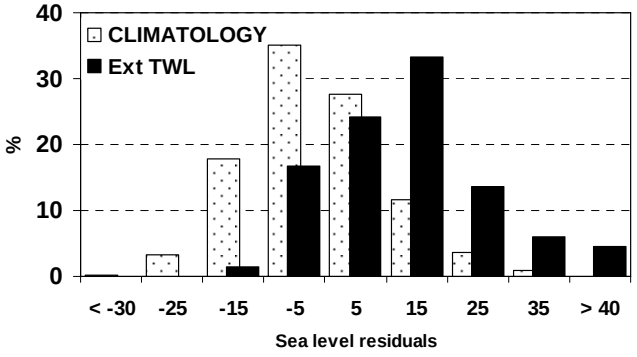

Fig. 6. Frequency of occurrence of meteorological sea level residuals during eTWL events (dark bar) and climatology (white bar) along the coast of northern Spain derived from instrumental data (Bilbao tide gauge, 1992–2008).

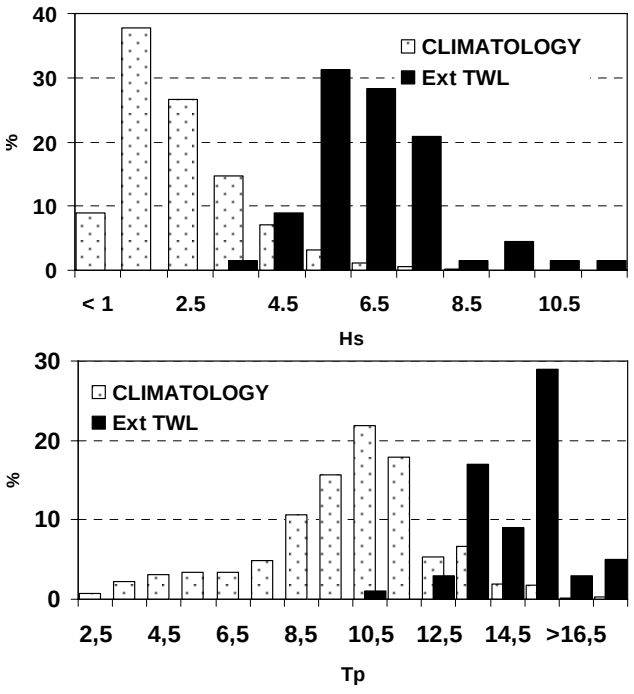

Fig. 7. Frequency of occurrence of significant wave heights (left) and wave peak periods (right) during eTWL events (dark bar) and climatology (white bar) along the coast of northern Spain derived from instrumental data (Bilbao buoy, 1992–2008).

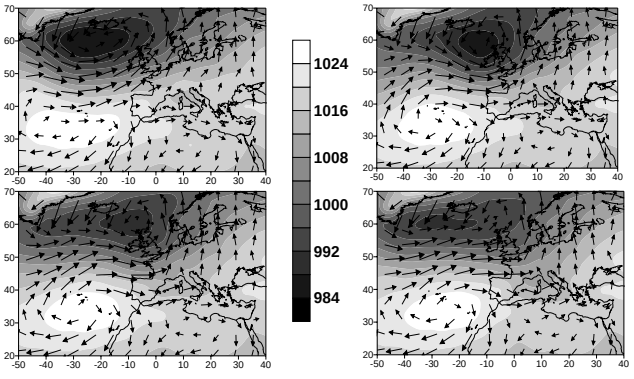

Fig. 8. Composites of SLP (hPa) and 10 m wind ($m\,s^{-1}$), performed for different time lags (48 h – upper left panel, 24 h – upper right panel, 12 h – low left panel and 0 h – low right panel) for independent extreme TWL events along the coast of northern Spain derived from instrumental data (1992–2008). The detached arrows are proportional to the wind speed.

residuals during eTWL events might be attributed to nearby weak cyclones, but this is not compatible with the observed highly significant heights and long periods of the waves. In fact, since waves grow continuously under the action of the wind, they depend on the overall wind stress along their complete path, thus high waves tend to reach the highest values not only where strong local winds are blowing (sea waves), but also when a long fetch is simultaneously present, specially where the coast is facing the prevailing surface winds. This swell component is largely determined by the frequency and intensity of remote extratropical disturbances, thus long wave periods usually indicate storm tracks passing far from the study area (Dupuis et al., 2006).

In order to confirm the hypothesis, composites of SLP and 10 m wind speed and directions were calculated for independent events during the reference period. Several time lags were chosen (48, 24, 12 and 0 h; Fig. 8) to explore if persistence was another relevant parameter to explain the previous characteristics of the eTWL events. All the figures highlight the role of well-known centres of action, such as the Icelandic Low and the Azores High, as well as an enhanced pressure gradient over the Bay of Biscay, driving strong westerly winds. However, their exact location and strength change as the eTWL event evolves. Simultaneously to the eastward movement of the main disturbance, located in the Northern Atlantic, a secondary low sometimes develops over the western Mediterranean (clearly seen at 24 or 12 time steps) which locally intensifies the pressure gradient over the Gulf of Biscay, which becomes more north-south oriented (Buzzi and Tibaldi, 1978; Alpert et al., 1990). The surface wind over the eastern Atlantic, associated with the SLP field described above, essentially maintains the large-scale westerly direction throughout the 48-h period, although the maximum wind area migrates from the central Atlantic towards Western Europe and veers from a south-westerly to a north-westerly component at the time of the highest TWL values.

The exact location of the storm minima during independent eTWL and their tracks are shown in Fig. 9. The track density of cyclones is greatest between Iceland and the British Isles, mostly extending from the North Atlantic well into Northern Europe. In correspondence with the displacement of the storms, the eTWL events occur when most of the pressure minimums are located between 50 and 70° N. On

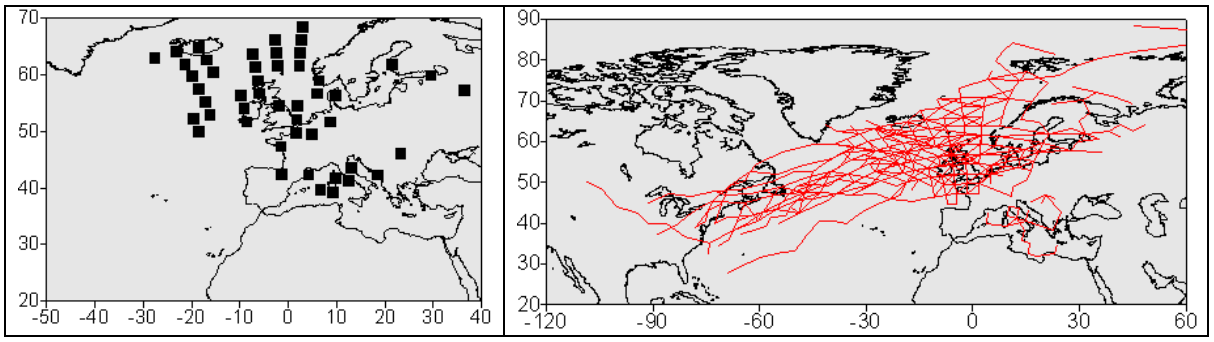

Fig. 9. Location of the storm pressure minimum and corresponding storm tracks for independent eTWL events along the coast of northern Spain derived from instrumental data (1992–2008).

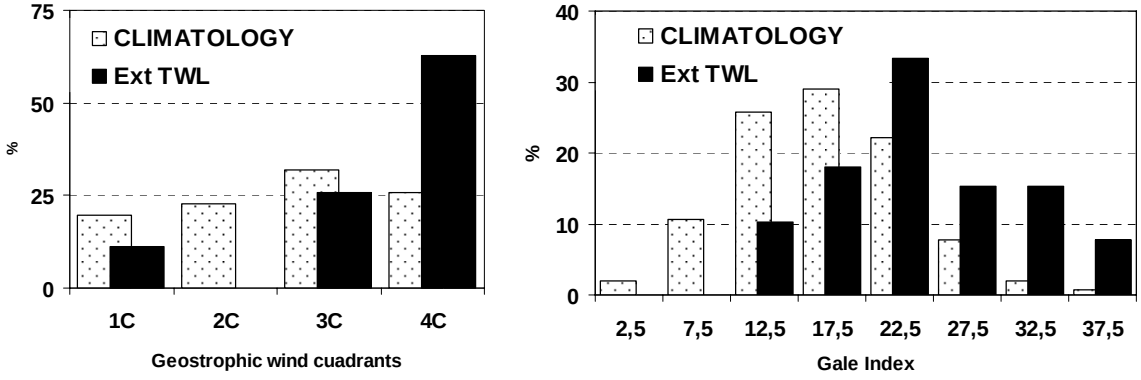

Fig. 10. Histograms of the: **(a)** frequency of geostrophic wind direction by quadrants and **(b)** values of the Gale Index (white bar October–March climatology; dark bar extreme TWL events) derived from instrumental data (1992–2008).

average, the intensity of the systems (Laplacian, not shown) is higher over the eastern North Atlantic, between the southern tip of Greenland, Iceland and British Isles. Thus most of the eTWL events occur when the systems enter into a decline phase, and consequently, when large scale winds that blow along their southern flank begin to reduce their strength.

At regional scale (Fig. 10), the geostrophic wind over the Bay of Biscay area acquires a predominant north-westerly component (most of the directions are comprised between 250° and 30°). The gale index magnitude is clearly stronger than the average values, since only during 28% of the events are weaker than 20 units, but this interval represents 67% of the days in the climatology.

5.3 Long-term trends of forcing processes

A statistical analysis of the variability and long-term trends (from October to March) of the total atmospheric forcing and its different components was carried out, the trends then being calculated as simple linear trends over the 44-yearly values. Five percentile values, namely the 99th percentile, 95th percentile, 75th percentile, 25th percentile and 5th percentile, and the average were used for the analysis. Their significance levels, obtained from a Kendall test, plus confidence intervals for the Sen's slope estimation, are shown in Tables 2, 3, 4 and 5. Only two single magnitudes showed significant trends: a generalized reduction of meteorological sea level residuals and an increasing trend of the wave period, while total atmospheric forcing and significant wave height do not show any trend over the 44 year period. Conversely, the corresponding time series of the total frequency and average persistence of the regional scale atmospheric circulation conditions (geostrophic wind $>250°$ and $<30°$ and Gale index >15 units) that might favour extreme TWL events show a slight reduction, not significant from the statistical point of view (Table 6).

Both trends can be understandable if the synoptic forcing is analyzed in terms of the frequency and strength of the north Atlantic cyclones. Recent research has shows that the Iberian Peninsula area has experienced a decline in storminess throughout the last quarter of the 20th century, with consequences for lower wind speeds and other variables (García-Herrera et al., 2007; Trigo et al., 2008); results from Brittany offer a similar picture of decrease in the frequency of atmospheric depressions and strong surge winds (Pirazzoli, 2000). Bearing in mind the preferred paths and locations of

Table 2. Statistical significance of the trends in the 99%, 95%, 75%, average, 25%, and 5% percentiles of the seasonal evolution (ONDJFM) of the total atmospheric forcing (sea surge plus wave run-up) calculated from SIMAR 44 (1958–2001).

Percentile time series	Mann-Kendall trend		Sen's slope estimate (value per year)				
	Test Z	Signific.	Q	Qmin99	Qmax99	Qmin95	Qmax95
99%	−0.419		−0.002	−0.011	0.011	−0.009	0.007
95%	0.502		0.001	−0.006	0.008	−0.004	0.006
75%	1.067		0.002	−0.003	0.006	−0.001	0.005
Average	0.921		0.001	−0.002	0.004	−0.001	0.004
25%	1.151		0.001	−0.002	0.004	−0.001	0.004
5%	−0.230		0.000	−0.004	0.003	−0.003	0.002

Table 3. Statistical significance of the trends in the 99%, 95%, 75%, average, 25%, and 5% percentiles of the seasonal evolution (ONDJFM) of meteorological sea level residuals values simulated by SIMAR 44 (1958–2001).

Percentile time series	Mann-Kendall trend		Sen's slope estimate (value per year)				
	Test Z	Signific.	Q	Qmin99	Qmax99	Qmin95	Qmax95
99%	−2.156	95%	−0.001	−0.003	0.000	−0.002	0.000
95%	−3.246	99%	−0.002	−0.003	0.000	−0.003	−0.001
75%	−2.355	95%	−0.001	−0.003	0.000	−0.002	0.000
Average	−2.721	99%	−0.001	−0.002	0.000	−0.002	0.000
25%	−2.398	95%	−0.001	−0.002	0.000	−0.001	0.000
5%	−1.739	90%	0.000	−0.001	0.000	−0.001	0.000

Table 4. Statistical significance of the trends in the 99%, 95%, 75%, average, 25%, and 5% percentiles of the seasonal evolution (ONDJFM) of significant wave height values simulated by SIMAR 44 (1958–2001).

Percentile time series	Mann-Kendall trend		Sen's slope estimate (value per year)				
	Test Z	Signific.	Q	Qmin99	Qmax99	Qmin95	Qmax95
99%	−0.807		−0.007	−0.033	0.025	−0.027	0.016
95%	−0.630		−0.004	−0.018	0.011	−0.015	0.007
75%	1.026		0.002	−0.004	0.007	−0.002	0.006
Average	0.910		0.000	−0.006	0.012	−0.003	0.010
25%	0.970		0.000	0.000	0.006	0.000	0.005
5%	0.701		0.000	0.000	0.004	0.000	0.003

Table 5. Statistical significance of the trends in the 99%, 95%, 75%, average, 25%, and 5% percentiles of the seasonal evolution (ONDJFM) of wave peak period values simulated by SIMAR 44 (1958–2001).

Percentiles time series	Mann-Kendall trend		Sen's slope estimate (value per year)				
	Test Z	Signific.	Q	Qmin99	Qmax99	Qmin95	Qmax95
99%	1.328		0.004	−0.005	0.016	0.000	0.013
95%	1.933	90%	0.011	−0.006	0.031	0.000	0.025
75%	2.310	95%	0.011	0.000	0.025	0.000	0.021
Average	1.988	95%	0.010	−0.002	0.024	0.000	0.021
25%	2.554	95%	0.017	0.000	0.034	0.003	0.031
5%	−0.052		0.000	−0.027	0.023	−0.021	0.019

Table 6. Statistical significance of the seasonal evolution (ONDJFM) of the atmospheric circulation conditions typical of eTWL along the northern coast of the Iberian Peninsula (1958–2001).

	Mann-Kendall trend		Sen's slope estimate (value per year)				
	Test Z	Signific.	Q	Qmin99	Qmax99	Qmin95	Qmax95
Frequency	−1.155		−0.065	−0.220	0.087	−0.178	0.053
Persistence	−0.418		−0.004	−0.030	0.022	−0.022	0.016
Sea level pressure	3.354	99.9%	0.108	0.030	0.178	0.051	0.162
Gale index	−0.109		−0.001	−0.025	0.021	−0.019	0.016

the cyclones responsible for extreme TWL events, two different categories were defined: a northernmost track, corresponding to cyclone cores crossing the −5° W meridian well above the 55° N parallel, and a southern track, when the same meridian is crossed between 40° N and 55° N. Cyclones using the northern track have increased their frequency and strength (Table 7), simultaneously with the dominant positive phase of the North Atlantic Oscillation since 1970 (Serreze et al., 1997), while the ones following the southern track have undergone significant decreases in frequency and strength. As an example of the behaviour of both classes of cyclones, we have selected the period from 15 to 20 February 2006, in which the northern coast of Spain suffered the effects of both types of cyclones (Fig. 11). The first one, tracking through the north Atlantic well above the 60° N, was the cause of a stormy period, characterized by swell conditions with maximum wave heights of more than 8 m and wave periods longer than 11 s around 17 February 06:00 UTC, a storm surge reached a maximum of 25 cm three hours later, when the significant wave height decreased to less than 7 m. Two days later, a new storm crossed the area, following a path through the Gulf of Biscay; maximum wave activity was measured about 12:00 UTC (significant wave height of 6.1 m and wave period of 8 s), after the cold front had crossed, when the geostrophic flow became northwesterly and sea level pressure was rising. The simultaneous storm surge was relatively low (16 cm) in comparison with values measured at 09:00 UTC (28 cm), when sea level pressure was falling, but the winds blew with an offshore (southerly) component.

Finally, astronomical tides and an annual rate of relative sea-level rise of 2.08 mm yr^{-1} (Marcos et al., 2005) was also applied to the 6-hourly values of the atmospheric forcing calculated from SIMAR 44 (Fig. 12) to simulate the long-term variability of TWL since 1958. A clear increasing trend in the frequency of occurrence of extreme TWL was obtained (dashed curve). However, if independent events are taking into account (solid curve), i.e. events separated by at least 48 h, the significance of the trend is reduced. This difference can be easily explained by more frequent secondary events, embedded within the same storm. Bearing in mind that the six-hour sampling of the data and the semi-diurnal tide regime of the region (high and low tides separated by a six hour time period) reduces the chances of additional extreme TWL within the same storm event, the observed trend should have underestimated the overall occurrence of extreme TWL.

Table 7. Statistical significance of the seasonal evolution (ONDJFM) of some cyclone magnitudes (1958–2001).

	Mann-Kendall trend		Sen's slope estimate (value per year)				
	Test Z	Signific.	Q	Qmin99	Qmax99	Qmin95	Qmax95
Northern Track							
Frequency	2.653	99%	1.429	0.021	2.750	0.412	2.518
Sea level presure	−1.522		−0.052	−0.160	0.053	−0.136	0.024
Laplacian	2.041	95%	0.027	−0.006	0.063	0.001	0.055
Southern Track							
Frequency	−2.050	95%	−0.955	−2.183	0.232	−1.810	−0.066
Sea level presure	3.078	99%	0.094	0.015	0.156	0.037	0.141
Laplacian	0.745		0.008	−0.022	0.038	−0.015	0.028

6 Discussion and conclusions

Assessing the geomorphological impact of storminess along the northern coast of the Iberian Peninsula is currently a challenging task. From the global sea level rise, which has been acknowledged as the most probable mechanism conductive to enhanced coastal erosion, changes in storm climate and human activities (Zhang et al., 2004), the latter is, by far, the main agent of morphological changes along the coast of northern Spain. For example, only about 20% of such changes along the Basque coast during the second half of the 20th century can be considered "natural" (without inclusion of recovery towards a naturalized state; Chust et al., 2010). Most of the coastline is characterized by cliffs on hard substrata (limestone, quarcite), making it difficult to detect, quantify and interpret actual geomorphological processes. Activities such as extraction of arid goods, forestry reforestation, and lately leisure and recreation activities, have deeply interfered with the dynamic of softer areas (beaches, dune fields), while estuaries, river mouths and bays, preferential areas for settlement, have experienced filling of the shallower sections or dredging of the deepest, which has changed the sedimentary budget. Additionally, variations in sediment supply might also have induced changes in some coastal areas, as a response to climate variability (riverflow changes) or human activities (construction of reservoirs, channelling). In conclusion, the current status of the coast is stable with a medium exposure, except along Cantabria, where the degree of exposure is higher (EUROSION, 2010).

However, although visualized as spotty patches, traces of active erosion do appear along the whole coast, affecting a wide variety of substratum through different processes: landslides and collapses on resistant materials (Alonso et al., 2000; Pagés et al., 2002; Flor and Flor-Blanco, 2005), which have affected even archaeological sites (Lorenzo et al., 2007); retreats or the complete loss of dune fields and soft cliffs (Rivas and Cendrero, 1994; Garzón and Garrote, 2004; Flor et al., 2004); spit collapses (Arteaga and González, 2005) or beach surface reduction (Chust et al., 2010). Quantification of rates of erosion has been attempted through photogrammetry procedures, but their link to storminess is difficult because the temporal frequency of the aerial surveys usually does not match the known changes in atmospheric circulation around the Iberian Peninsula.

Our approach assumes that, although disperses, such evidence is the reflection of a natural evolution of the coastline. Consequently, this paper discusses whether they might be related either to an increase in storminess or a result of the increased water sea levels, or a combination of both. First of all, episodes of potential erosion were identified through the calculation of the extreme (1%) Total Water Levels using instrumental observations of sea level and wave activity. Then, a characterization of the oceanographic parameters associated with those events was followed by an examination of the atmospheric circulation conditions leading to them. Finally, an analysis of the long-term trends in the oceanographic (based on a 44-year hindcasted database) and atmospheric conditions (NCEP Reanalysis) was performed.

Typical oceanographic features of the episodes of extreme TWL in our study region are rough wave conditions (large significant heights and long waves) and moderate, above normal sea level atmospheric residuals. Conversely, the most relevant atmospheric features of those events are deep extratropical lows, usually following a northern path, northward the 50° N parallel, developing strong and persistent westerly winds over time. The long fetch supports swell conditions and moderate storm surges, the latter is mainly caused by the onshore wind stress over the water surface, although the short continental shelf reduces their magnitude.

A long-term analysis of the atmospheric circulation shows that local conditions have evolved to a reduction of the number and strength of the atlantic storms, However, such conditions have been balanced by the favourable exposition of the northern coast of the Iberian Peninsula to the increasing

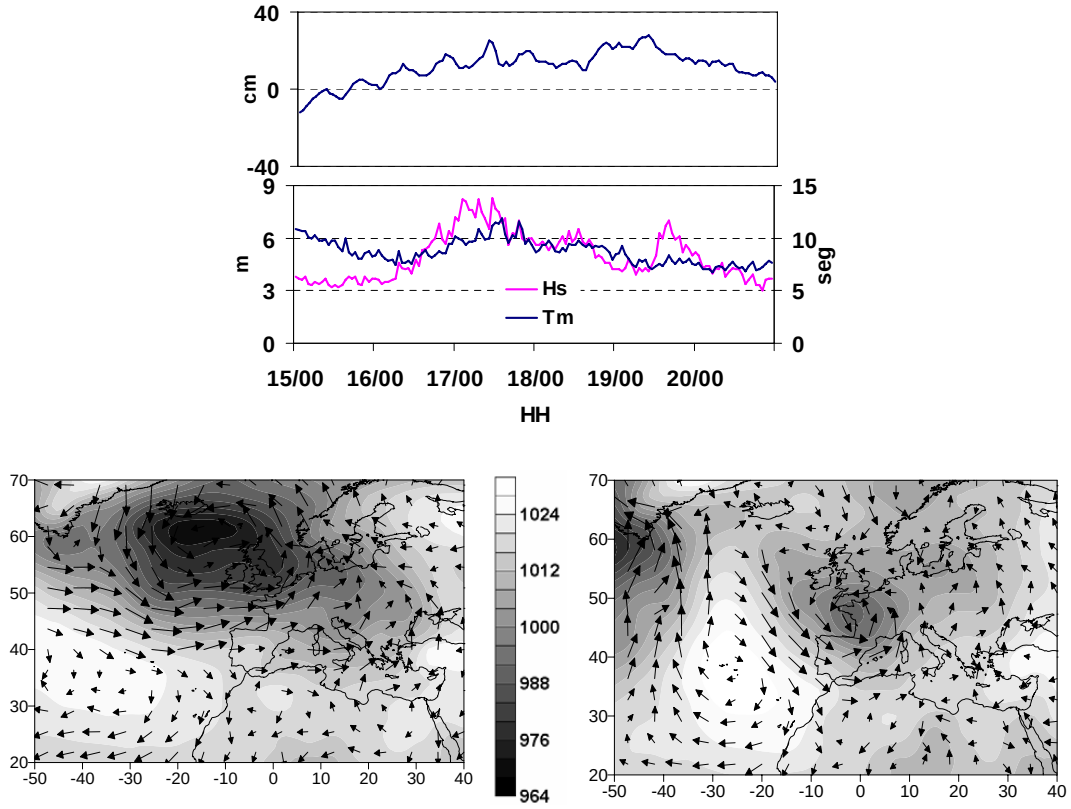

Fig. 11. Evolution of sea level anomalies (upper panel), significant wave height and wave period (middle panel) from 15 to 20 February 2006. Sea level pressure and surface wind speed and direction (lower panel) corresponding to 17 February 2006 at 06:00 UTC (left) and 19 February 2006 at 12:00 UTC.

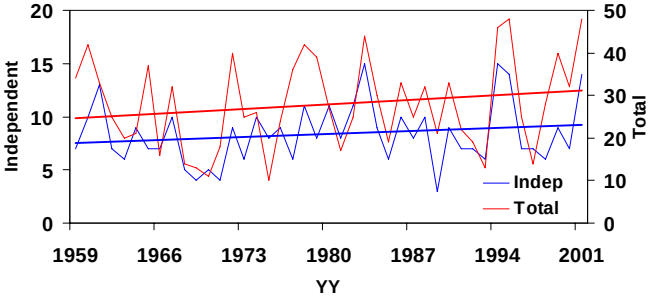

Fig. 12. Long term trends of occurrence of eTWL events (total events, red line; independent events, blue line) along the coast of northern Spain derived from SIMAR 44.

frequency and strength of distant disturbances. As a consequence, the long-term variability of oceanographic parameters obtained from the SIMAR 44 hindcast database shows that the atmospheric forcing component of the Total Water Level values (meteorological sea level residuals plus wave run up) have not changed over the available period of data; the decreasing trend of the meteorological sea level residuals has been compensated by longer wave peak periods. Although the results obtained from the analysis of wave peak period must be treated with some caution, since this variable is not as well simulated by SIMAR 44 as by SWH (Pilar et al., 2008), both trends are in agreement with the local and large scale atmospheric circulation trends mentioned above and supported by recent research on long-term trends of wave parameters (Dupuis et al., 2006; Dodet et al., 2010). Finally, the addition of the rate of relative sea level trend to the temporal evolution of the atmospheric forcing component of the Total Water Level values is enough to simulate more persistent eTWLs, which might explain some of the evidence of current erosive processes along the coast of northern Spain.

Acknowledgements. This research was funded by a Spanish Science and Technology CICYT research project (CGL2007-65546-C03-03/CLI (lBERSYNOP) “Caracterización sinóptica de la circulación atmosférica secular sobre la Península Ibérica”). The Spanish Goverment Agency “Puertos del Estado” is acknowledged for providing the observed and simulated database, and NOAA/ESRL Physical Sciences Division for providing NCEP Reanalysis database. Many thanks also to the anonymous reviewers whose useful comments and suggestions have greatly improved the final manuscript.

Edited by: J. Salat
Reviewed by: J. A. Jimenez and another anonymous referee

References

Alonso, A., Lorenzo, F., and Pagés, J. L.: Dinámica litoral y erosión en la Ria de O Barqueiro: factores antrópicos y procesos naturales, Geogaceta, 28, 7–10, 2000.

Alpert, P., Neeman, B. U., and Shay-El, Y.: Climatological analysis of Mediterranean cyclones using ECMWF data, Tellus, 42A, 65–77, 1990.

Álvarez, E., Rodríguez, I., and Pérez, B.: A description of the tides in the Eastern North Atlantic, Prog. Oceanogr., 40, 217–244, 1997.

Álvarez-Fanjul, E., Pérez, B., and Rodríguez, I.: Nivmar: a storm surge forecasting system for Spanish waters, Sci. Mar., 65, 145–154, 2001.

Arteaga, C. and González, J. A.: Natural and Human Erosive Factors in Liencres Beach Spit and Dunes (Cantabria, Spain), J. Coastal Res., SI 49 (Proceedings of the 2nd Meeting in Marine Sciences), 70–75, 2005.

Borja, A. and Collins, M.: Oceanography and Marine Environment of the Basque Country, Elsev. Oceanogr. Series, 204 pp., 2004.

Buzzi, A. and Tibaldi, S.: Cyclogenesis in the lee of Alps: a case study, Q. J. Roy. Meteor. Soc., 104, 271–287, 1978.

Chust, G., Borja, A., Liria, P., Galparsoro, I., Marcos, M., Caballero, A., and Castro, R.: Human impacts overwhelm the effects of sea-level rise on Basque coastal habitats (N Spain) between 1954 and 2004, Estuar. Coast. Shelf S., 84, 453–462, 2010.

Costanza, R., d'Arge, R., de Groot, R., Farber, S., Grasso, M., Hannon, B., Limburg, K., Naeem, S., O'Neill, R. V., Paruelo, J., Raskin, R. G., Sutton, P., and van den Belt, M.: The value of the world's ecosystem services and natural capital, Nature, 387, 253–260, 1997.

Crooks, S.: The effect of sea-level rise on coastal geomorphology, Ibis, 146, 18–20, 2004.

Denslow, J. S. and Battaglia, L. L.: Stand composition and structure across a changing hydrologic gradient: Jean Lafitte National Park, Louisiana, USA, Wetlands, 22, 738–752, 2002.

Desantis, L. R. G., Bhotika, S., Williams, K., and Putz, F. E.: Sea-level rise and drought interactions accelerate forest decline on the Gulf Coast of Florida, USA, Glob. Change Biol., 13, 2349–2360, 2007.

Dodet, G., Bertin, X., and Taborda, R.: Wave climate variability in the North-East Atlantic Ocean over the last six decades, Ocean Model., 31, 120–131, 2010.

Dupuis, H., Michel, D., and Sottolichio, A.: Wave climate evolution in the Bay of Biscay over two decades, J. Marine Syst., 63, 105–114, 2006.

EUROSION: Living with coastal erosion in Europe. Sand and Space for Sustainability. Guidance document for quick hazard assessment of coastal erosion and associated flooding, available at: http://www.eurosion.org/reports-online/reports.html, last access: 21 October 2010.

FitzGerald, D. M., Fenster, M. S., Argow, B. A., and Buynevich, I. V.: Coastal impacts due to sea-level rise, Annu. Rev. Earth Pl. Sc., 36, 601–647, 2008.

Flor, G. and Flor-Blanco, G.: An introduction to the erosion and sedimentation problems in the coastal regions of Asturias and Cantabria (NW Spain) and its implications on environmental management, J. Coastal Res., SI 49 (Proceedings of the 2nd Meeting in Marine Sciences), 58–63, 2005.

Flor, G., Flor-Blanco, G., and and Martínez, J. F.: Evolución del campo dunar de El Puntal (Laredo), in: Procesos geomorfológicos y evolución costera, edited by: Blanco, R., López, J., and Pérez Alberti, A., Santiago de Compostela, University Press, 155–166, 2004.

García-Herrera, R., Paredes, D., Trigo, R. M., Trigo, I. F., Hernández, H., Barriopedro, D., and Mendes, M. A.: The outstanding 2004-2005 drought in the Iberian Peninsula: associated atmospheric circulation, J. Hydrometeorol., 8, 483–498, 2007.

Garzón, M. G. and Garrote, H. J.: Análisis del retroceso del frente de la costa usando fotogramas aéreos, Oyambre (Cantabria), in: Procesos geomorfológicos y evolución costera: actas de la II Reunión de Geomorfología Litoral, edited by: Blanco, R., López, J., and Pérez, A., 51–66, 2004.

Guedes-Soares, C., Weisse, R., Carretero, J. C., and Álvarez-Fanjul, E.: A 40 years hindcast of wind, sea level and waves in European waters, Proc. 21st Int. Conf. on Offshore Mechanics and Arctic Engineering, ASME, Oslo, Paper OMAE2002-28604, 2002.

Goda, Y.: On the methodology of selecting design wave height, in: Proceedings of the 21st International Conference on Coastal Engineering, edited by: Edge, B. L., Malaga, American Society of Civil Engineers, 899–913, 1988.

González, M., Uriarte, A., Fontán, A., Mader, J., and Gyssels, P.: Marine dynamics, in: Oceanography and Marine Environment of the Basque Country, edited by: Borja, A. and Collins, M., Elsev. Oceanogr. Series, 70, 133–157, 2004.

Iglesias, G. and Carballo, R.: Offshore and inshore wave energy assessment: Asturias (N Spain), Energy, 35, 1964–1972, 2010.

Jenkinson, A. and Collison, F.: An initial climatology of gales over the North Sea areas, Synoptic Climatology Branch Memorandum no 62, Met Office, Bracknell, 1977.

Jokiel, P. L. and Brown, E. K.: Global warming, regional trends and inshore environmental conditions influence coral bleaching in Hawaii, Glob. Change Biol., 10, 1627–1641, 2004.

Kalnay, E., Kanamitsu, M., Cistler, R., Collins, W., Deaven, D., Gandin, L., Iredell, M., Saha, S., White, G., Woollen, J., Zhu, Y., Chelliah, M., Ebisuzaki, W., Higgins, W., Janowiak, J., Mo, K., Ropelewski, C., Wang, J., Leetma, A., Reynolds, R., Jenne, R., and Joseph, D.: The NCEP/NCAR 40-year reanalysis project, B. Am. Meteorol. Soc., 77, 437–471, 1996.

Kushnir, Y., Cardone, V. J., Greenwood, V. G., and Cane, M. A.: The recent increase in North Atlantic wave heights, J. Climate, 10, 2107–2113, 1997.

Leorri, E. and Cearreta, A.: Recent sea-level changes in the southern Bay of Biscay: transfer function reconstructions from salt-marshes compared with instrumental data, Sci. Mar., 73(2), 287–296, 2009.

Lorenzo, F., Alonso, A., and Pagés, J. L.: Erosion and Accretion of Beach and Spit Systems in Northwest Spain: A Response to Human Activity, J. Coastal Res., 23(4), 834–845, 2007.

Marcos, M., Gomis, D., Monserrat, S., Álvarez-Fanjul, E., Pérez, B., and García-Lafuente, J.: Consistency of long sea-level time series in the northern coast of Spain, J. Geophys. Res., 110, C03008, doi:10.1029/2004JC002522, 2005.

Marcos, M., Wöppelmann, G., Bosch, W., and Savcenko, R.: Decadal sea level trends in the Bay of Biscay from tide gauges, GPS and TOPEX, J. Marine Syst., 68(3–4), 529–536, 2007.

Meehl, G. A., Stocker, T. F., and Collins, W. D.: Global Climate Projections, in: Contribution of Working Group I to the Fourth Assessment Report of the Intergovernmental Panel on Climate

Change, Climate Change 2007: The Physical Science Basis, edited by: Solomon, S., Qin, D., and Manning, M., Cambridge University Press, 749–844, 2007.

Méndez, F. J., Menéndez, M., Luceño, A., and Losada, I. J.: Estimation of the long-term variability of extreme significant wave height using a time-dependent Peak Over Threshold (POT) model, J. Geophys. Res., 111, C07024, doi:10.1029/2005JC003344, 2006.

Michael, J. A.: Episodic flooding and the cost of sea-level rise, Ecol. Econ., 63, 149–159, 2007.

Morata, A., Luna, M. Y., Martín, M. L., Sotillo, M. G., and Valero, F.: Iberian autumnal precipitation characterization through observed, simulated and reanalysed data, Adv. Geosci, 16, 49–54, 2008.

Pagés, J. L., Lorenzo, F., and Alonso, A.: Procesos erosivos en la Estaca de Bares y la Ria de O Barqueiro (A Coruña—Lugo), in: Estudios recientes en Geomorfología, SEG, Valladolid, Spain, Univ de Valladolid, 373–382, 2002.

Pascual, A., Cearreta, A., Rodríguez-Lázaro, J., and Uriarte, A.: Geology and palaeoceanography, in: Oceanography and Marine Environment of the Basque Country, edited by: Borja, A. and Collins, M., Elsev. Oceanogr. Series, 70, 53–73, 2004.

Pilar, P., Guedes-Soares, C., and Carretero, J. C.: 44-year wave hindcast for the North East Atlantic European coast, Coast. Eng., 55, 861–871, 2008.

Ratsimandresy, A. W., Sotillo, M. G., Carretero, J. C., Álvarez-Fanjúl, E., and Hajji, H.: A 44-year high-resolution ocean and atmospheric hindcast for the Mediterranean Basin developed within the HIPOCAS Project, Coast. Eng., 55, 827–842, 2008.

Pirazzoli, P. A.: Surges, atmospheric pressure and wind change and flooding probability on the Atlantic coast of France, Oceanol. Acta, 23, 643–661, 2000.

REDMAR: Resumen de parámetros relacionados con el nivel del mar y la marea que afectan a las condiciones de diseño y explotación portuaria, Organismo Público Puertos del Estado, Madrid, 2005.

Rivas, V. and Cendrero, A.: Human influence in a low-hazard coastal area: an approach to risk assessment and proposal of mitigation strategies, J. Coastal Res., 12, 289–298, 1994.

Ruggiero, P., Komar, P. D., McDougal, W. G., and Beach, R. A.: Extreme water levels, wave runup, and coastal erosion, Proc. 25th Coastal Engineering Conf., ASCE, 2793–2805, 1996.

Ruggiero, P., Kaminsky, G., Komar, P. D., and McDougal, W. G.: Extreme Waves and Coastal Erosion in the Pacific Northwest, in: Waves '97: Third Symposium on Ocean Wave Measurement and Analysis, Virginia Beach, 947–961, 1997.

Ruggiero, P., Komar, P. D., McDougal, W. G., Marra, J. J., and Beach, R. A.: Wave runup, extreme water levels and the erosion of properties backing beaches, J. Coastal Res., 17(2), 407–419, 2001.

Ruggiero, P., Holman, R. A., and Beach, R. A.: Wave runup on a high-energy dissipative beach, J. Geophys. Res., 109, C06025, doi:10.1029/2003JC002160, 2004.

Schrötter, D., Cramer, W., and Leemans, R.: Ecosystem service supply and vulnerability to global change in Europe, Sciencexpress, 27, 1–4, 2005.

Sebastião, P., Guedes-Soares, C., and Álvarez, E.: 44 years hindcast of sea level in the Atlantic Coast of Europe, Coast. Eng., 55, 843–848, 2008.

Serreze, M. C.: Climatological aspects of cyclone development and decay in the Arctic, Atmos. Ocean, 33, 1–23, 1995.

Serreze, M. C., Carse, F., Barry, R. G., and Rogers, J. C.: Icelandic Low cyclone activity: Climatological Features, linkages with the NAO and relationships with recent changes in the Northern Hemisphere Circulation, J. Climate, 10(3), 453–464, 1997.

Sotillo, M. G., Ratsimandresy, A. W., Carretero, J. C., Bentamy, A., Valero, F., and González-Rouco, J. F.: A high-resolution 44-year atmospheric hindcast for the Mediterranean Basin: Contribution to the regional improvement of global reanalysis, Clim. Dynam., 25, 219–236, 2005.

Sotillo, M. G., Aznar, R., and Valero, F.: Mediterranean offshore extreme wind analysis from the 44-year HIPOCAS database: different approaches towards the estimation of return periods and levels of extreme values, Adv. Geosci., 7, 275–278, 2006, http://www.adv-geosci.net/7/275/2006/.

Stockdon, H. F., Holman, R. A., Howard, P. A., and Sallenger, A. H.: Empirical parameterization of setup, swash, and runup, Coast. Eng., 53, 573–588, 2006.

Trigo, R. M., Valente, M. A., Trigo, I. F., Miranda, P. M., Ramos, A. M., Paredes, D., and García-Herrera, R.: The impact of Morth Atlantic wind and cyclone trends on European precipitation and significant wave height in the Atlantic, Ann. NY Acad. Sci., 1146, 212–234, 2008.

Turner, R. K., Subak, S., and Adger, W. N.: Pressures, Trends, and Impacts in Coastal Zones: Interaction between socio-economic and natural systems, Env. Manag., 20, 159–173, 1996.

Wang, X. L. and Swail, V. R.: Trends of Atlantic Wave Extremes as Simulated in a 40-Yr Wave Hindcast Using Kinematically Reanalyzed Wind Fields, J. Climate, 15, 1020–1035, 2001.

Hasselmann, S., Hasselmann, K., Bauer, E., Janssen, P. A. E. M., Komen, G. J., Bertotti, L., Lionello, P., Guillaume, A., Cardone, V. C., Greenwood, J. A., Reistad, M., Zambresky, L., and Ewing, J. A. (WAMDI Group): The WAM Model – A third generation ocean wave prediction model, J. Phys. Oceanogr., 18, 1775–1810, 1988.

WASA Group: Changing waves and storms in the northeast Atlantic, B. Am. Meteorol. Soc., 79, 741–760, 1998.

Williams, K., Ewel, K. C., Stumpf, R. P., Putz, F. E., and Workman, T. W.: Sea-level rise and coastal forest retreat on the west coast of Florida, USA, Ecology, 80, 2045–2063, 1999.

Williams, K., McDonald, M., and Sternberg, L.: Interactions of storm, drought, and sea-level rise on coastal forest: a case study, J. Coastal Res., 19, 1116–1121, 2003.

Yarnal, B.: Synoptic climatology in environmental analysis: a primer, Belhaven Press, London, 1993.

Zhang, K., Douglas, B. C., and Leatherman, S. P.: Global warming and coastal erosion, Climatic Change, 64, 41–58, 2004.